Journal of Agricultural Engineering

https://www.agroengineering.org/

A test for monitoring erosion on the Cape Fear experimental hillslope using a low-cost camera

Andrea Petroselli,[1] Ettore Arcangeletti,[1] Ciro Apollonio,[1] Flavia Tauro,[2] Salvatore Grimaldi[2]

[1]Department of Agriculture and Forest Sciences (DAFNE);
[2]Department for Innovation in Biological, Agro-Food and Forest Systems (DIBAF), Tuscia University, Viterbo, Italy

Corresponding author: Andrea Petroselli, Department of Agriculture and Forest Sciences (DAFNE), Tuscia University, Via San Camillo de Lellis snc, 01100 Viterbo, Italy. E-mail: petro@unitus.it

Please cite this article as doi: 10.4081/jae.2025.1786

Submitted: 23 March 2025
Accepted: 4 July 2025

A test for monitoring erosion on the Cape Fear experimental hillslope using a low-cost camera

Andrea Petroselli,[1] Ettore Arcangeletti,[1] Ciro Apollonio,[1] Flavia Tauro,[2] Salvatore Grimaldi[2]

[1]Department of Agriculture and Forest Sciences (DAFNE);

[2]Department for Innovation in Biological, Agro-Food and Forest Systems (DIBAF), Tuscia University, Viterbo, Italy

Corresponding author: Andrea Petroselli, Department of Agriculture and Forest Sciences (DAFNE), Tuscia University, Via San Camillo de Lellis snc, 01100 Viterbo, Italy. E-mail: petro@unitus.it

Contributions: all the authors made a substantive intellectual contribution, read and approved the final version of the manuscript and agreed to be accountable for all aspects of the work.

Conflict of interest: the authors declare no competing interests, and all authors confirm accuracy.

Acknowledgements: This study was carried out within the Agritech National Research Center and received funding from the European Union Next-GenerationEU (PIANO NAZIONALE DI RIPRESA E RESILIENZA (PNRR)—MISSIONE 4 COMPONENTE 2, INVESTIMENTO 1.4—D.D. 1032 17/06/2022, CN00000022). This manuscript reflects only the authors' views and opinions, neither the European Union nor the European Commission can be considered responsible for them.

Abstract

Remote sensing and image analysis are gaining popularity as low-cost, continuous alternatives to traditional soil erosion measurement methods. This technical note presents a comparison between direct erosion measurements and image-based estimates on a semi-natural hillslope, taken before and after an artificial rainfall event. Although discrepancies between the two methods ranged from 18% to 27%, the image-based approach successfully detects rills as small as 5-7 cm, highlighting its potential for real-time, continuous monitoring in field applications.

Introduction

Soil erosion is a significant environmental issue, impacting ecosystems by reducing soil fertility, agricultural productivity, and water quality, while contributing to habitat degradation and increased flood risks (Tan and Kuebbing, 2023). It also destabilizes riverbanks, harms biodiversity, and disrupts aquatic ecosystems (Maxwell *et al.*, 2019). Additionally, soil erosion plays a crucial role in watershed dynamics, especially in hillslopes and headwater regions, where rainfall-runoff transformation involves both distributed and concentrated erosion mechanisms. These processes alter drainage networks and slopes, impacting flood propagation and terrain stability. This underscores the need for effective, low-cost methods to monitor soil erosion in a spatially distributed and continuous manner, ideally in real time.

Various techniques are used to assess soil erosion, including direct and indirect methods (Nicosia *et al.*, 2024). Direct methods, while accurate, involve physically capturing eroded material over time, making them labor-intensive, costly, and unsuitable for large-scale or continuous monitoring (Todisco *et al.*, 2012; Pampalone *et al.*, 2024). In contrast, indirect methods, particularly those utilizing image analysis, are gaining traction for mapping and quantifying soil erosion patterns, rates, and spatial variability (Žížala *et al.*, 2017; Sánchez-Crespo *et al.*, 2023).

Over time, image analysis techniques have proven effective in enhancing our understanding of soil erosion. For example, Vinci *et al.* (2017) employed an Apple iPhone 6 Plus camera for Structure from Motion (SfM) photogrammetry to quantify soil erosion by assessing surface elevation changes caused by rainfall. Fernández Rodríguez *et al.* (2022) used a Huawei phone to capture images during a runoff test, demonstrating SfM's cost-effectiveness and reliability. Ehrhardt *et al.* (2022) applied a Samsung WB750 camera to reconstruct soil surfaces before and after rainfall events. Palmeri *et al.* (2024) utilized a GoPro Hero4 camera to survey rills over several years in Sicily. Image analysis has also been applied in river and headwater monitoring, offering valuable insights into flow velocity and water level variations (Manfreda *et al.*, 2024).

In previous work on image analysis techniques, we have tested various low-cost camera systems for estimating flow velocity and water levels to develop an integrated prototype for simultaneous discharge and soil erosion monitoring in ephemeral streams (Noto *et al.*, 2022; Tauro *et al.*, 2022). In this context, this study presents a feasibility test to assess whether soil erosion monitoring can be performed using low-cost, durable instrumentation, for integration into real-time monitoring systems for headwater regions. Specifically, the test evaluates (i) the accuracy of soil erosion estimation with a low-cost camera, and (ii) the ability of image analysis to detect and monitor micro-rills. A proof-of-concept experiment was conducted on a semi-natural hillslope under controlled conditions.

In particular, the objective of the present technical note is to evaluate the feasibility of using low-cost instrumentation for soil erosion monitoring, with a focus on assessing the accuracy of erosion estimates from a low-cost camera and the capability of image analysis to detect and monitor micro-rills.

Materials and Methods

In the following, the experimental hillslope (referred to as Cape Fear; Tauro *et al.*, 2017) is first introduced, followed by a detailed explanation of the image acquisition procedure and the DEM construction process.

Cape Fear experimental hillslope is a seminatural plot situated at the outdoor experimental farm of the University of Tuscia in Viterbo, Italy. The plot consists of 30 m^3 of natural wedge-shaped soil, as shown in Figure 1. The wedge covers a square area of 7×7 m^2 and is supported by a containment structure made of wooden boards and poles on three sides. It also has a foundation of an additional 10 m^3 of soil, which is isolated from the underlying ground by a waterproof plastic layer. To characterize the experimental hillslope soil, five undisturbed soil cores (0.07 m in length and 0.072 m in diameter) were collected from a depth of 0.05-0.12 m. On average, soil composition consists of 44% sand, 36% silt, and 20% clay. The saturated water content across the five samples ranged from 50% to 57%, with an average value of 54.4%.

Cape Fear facilitates experiments using both natural and artificial rainfall. To simulate artificial rainfall, the plot is equipped with four pressurized nozzle rainfall simulators, each outfitted with one pressure probe. Rainfall intensities can range from a minimum of 40 mm/h, achieved by using two small nozzles, to more than 200 mm/h when all three nozzles present on each rainfall simulator are activated simultaneously, depending on the pressure head.

Soil moisture, runoff, and turbidity are continuously monitored at a frequency of 1 Hz. Surface and subsurface runoff are collected in a V-shaped aluminum channel placed at the base of the plot. The runoff is directed into an aluminum tank, which consists of three interconnected compartments. This tank houses a stainless-steel OBS-3+ turbidity sensor and a structural testing system with a strain gauge. Finer solid materials and water levels are continuously measured by the sensors, while coarser solid materials are retained in the first compartment of the tank.

Monitored parameters are automatically recorded by a CR10X Campbell Scientific data logger and are then averaged to provide data at a 5-minute resolution. Detailed soil characterization, as well as the calibration of sprinklers, turbidity and water level sensors, have been previously documented in Tauro *et al.* (2017), Petroselli and Tauro (2017), and Tauro *et al.* (2023).

Cape Fear images were captured before and after a simulated rainfall event using a remote-controlled Sony ILCE QX1 camera, equipped with a 16 mm fixed lens. The camera was mounted on an extendable aluminum telescopic pole, which was extended to a height of 6 meters during recordings.

Before data processing, 14 Ground Control Points (GCPs) (Figure 2) were placed on the external surface of Cape Fear's containment structure, using threaded screws and washers that were pre-painted to enhance contrast. The topographic survey was conducted with a Topcon total station to accurately determine the coordinates.

The first photographic dataset was acquired on July 19, 2023, before the artificial rainfall event. Photos were taken approximately 1 meter apart, covering the perimeter of Cape Fear's experimental area while avoiding interference with the ground surface (Figure 2).

Frames were processed using Agisoft Metashape SfM software. The workflow began with the creation of a sparse point cloud, calibrated and georeferenced using GCPs from topographic surveys. A dense point cloud was then generated, providing a more detailed reconstruction, followed by the interpolation of a DEM. To ensure accuracy, foreign elements (e.g., rainfall simulators) were removed from the point cloud to prevent DEM distortions. For instance, in the case of rainfall simulators, their prominent height relative to the hillside surface makes them easily identifiable within the scene. As a result, their detection and subsequent removal from the point cloud is straightforward and can be manually carried out with precision using Agisoft Metashape's SfM software.

After the initial acquisition, a 4-hour rainfall event, characterized by an average rainfall intensity equal to 156 mm/h, was simulated using irrigation sprinklers. The process of image acquisition was then repeated for the post-event dataset (still on July 19, 2023). Both DEMs were cropped to the same mask, and a raster calculator was used to compute elevation differences.

Results

The test is evaluated through both quantitative and qualitative assessments. Quantitative analysis compares the weight of eroded material estimated by image analysis to the weight of eroded soil. Qualitative assessment involves visual analysis to determine whether the test can identify micro-rills formed after the artificial rainfall event.

Regarding quantitative results, Figure 3a and 3b shows the DEMs generated before and after the artificial rainfall event, while Figure 3c presents the raster of elevation differences. As shown in Figure 3c, areas of deposition (in green, up to a maximum of 3.5 cm) and areas of erosion (in brown, up to a maximum of 7 cm) are observed within the study area.

From Figure 3c, by summing the differential values for each individual pixel of the raster and multiplying by the unit surface area of the pixel, it is possible to determine a total eroded volume equal to 221,593 cm^3. This value represents the total volume of soil and pores containing both water and air. To obtain the volume of the soil alone, the volume of the soil pores must be excluded from the total volume. The volume of the soil pores can be estimated by assuming a porosity slightly greater than the saturation moisture content. In general, soil porosity sets an upper limit on the amount of water the soil can retain. However, the saturation moisture content may be lower than the porosity if some pores are too small to effectively hold water (as with microscopic pores) or too large to retain water due to drainage. Given Cape Fear average saturated water content of 54.4%, a soil porosity in the range of 50%-55% is here assumed.

Based on this, the total volume of eroded soil (excluding pores) is estimated to range from 110,797 cm^3 (assuming a soil porosity of 50%) to 99,717 cm^3 (assuming a soil porosity of 55%). The next step is to multiply these volumes by the specific weight of dry soil to obtain the estimated soil weight from image analysis. The specific weight of the dry soil can be determined from its composition (44% sand, 36% silt, 20% clay), assuming specific weights of 1.5 g/cm^3 for sand, 1.4 g/cm^3 for silt, and 1.3 g/cm^3 for clay (Brady, 1990). This gives an average specific weight of 1.42 g/cm^3. Finally, by multiplying the total volume of eroded soil (excluding pores) by the average specific dry weight, the image-based estimated soil weight ranges from 157.73 kg (assuming soil porosity of 50%) to 141.96 kg (assuming soil porosity of 55%).

The weight of the eroded soil obtained through image analysis is compared to the weight calculated using the traditional sediment collection method from the Cape Fear aluminum tank. Specifically, material collected in the first compartment of the aluminum tank, which refers to the coarser material, was dried at 105°C for 24 hours before being weighed. The resulting weight is 118.1 kg. To this value, we add the soil weight determined from the turbidity sensor, which is based on the recorded soil turbidity and the liquid runoff exiting the aluminum tank, referring to the finer material. This value is 76.3 kg, bringing the total weight of the solid material to 194.4 kg.

As results show, the two estimated dry weight values from the image analysis method (157.73 kg assuming a porosity of 50% and 141.96 kg assuming a soil porosity of 55%) are comparable to the direct measurement, with errors ranging from 18% to 27%, depending on the assumed porosity.

Regarding the qualitative results, the formation of several micro-rills is clearly observable in the upper portion of Figure 3, where visible surface alterations indicate concentrated flow paths induced by the artificial rainfall event. A closer examination is provided in Figure 4: panel (a) illustrates the pre-event surface conditions, while panel (b) shows the same area after the rainfall simulation, highlighting the emergence and deepening of rill structures. Panel (c) presents a differential analysis between the pre-event and post-event Digital Elevation Models (DEMs), effectively visualizing areas of sediment removal and deposition. In particular, Figure 4 reveals erosion features reaching depths of up to 7 cm, as well as deposition areas with accumulations up to 3.5 cm in height.

Together, these images offer compelling visual evidence that the image-based analysis approach employed in this study is capable of detecting and monitoring micro-rill development with a high level of detail and spatial resolution.

Conclusions

The present technical note aimed to assess the feasibility of using a low-cost camera for monitoring soil erosion, both quantitatively and qualitatively. The experiment was conducted on an artificial hillslope, analyzing erosion effects before and after a controlled rainfall event.

By comparing data from traditional direct erosion measurements to image-based analysis, we found that the latter provides a detailed and comprehensive representation of the soil erosion process. Results are promising, with discrepancies ranging from 18% to 27% compared to conventional methods. Furthermore, the applied methodology successfully identified micro-rills formed as a consequence of the erosion process triggered by rainfall events.

This experiment represents a preliminary step toward the development of a prototype integrating multiple monitoring capabilities for ephemeral headwaters. Future research will focus on replicating the test using the same camera and hardware components intended for the prototype under development. Additionally, different environmental sites will be tested to simulate real-field conditions, allowing us to evaluate potential performance variations in erosion estimation, with particular attention to the detection and characterization of micro-rills.

References

Brady, N.C. 1990. The nature and properties of soils, 10th ed. New York, Macmillan Publishing Co.

Ehrhardt, A., Deumlich, D., Gerke, H.H. 2022. Soil surface micro-topography by structure-from-motion photogrammetry for monitoring density and erosion dynamics. Front. Environ. Sci. 9:737702.

Fernández Rodríguez, R., Ponte, M., Bento, R., Cardoso, R. 2022. Potential of mobile application based on structure from motion (SfM) photogrammetry to monitor slope fast erosion by runoff water. Catena 216:106359.

Manfreda, S., Miglino, D., Saddi, K.C., Jomaa, S., Eltner, A., Perks, M., et al. 2024. Advancing river monitoring using image-based techniques: challenges and opportunities. Hydrol. Sci. J. 69:657-677.

Maxwell ,C.M., Langarudi, S.P., Fernald, A.G. 2019. Simulating a watershed-scale strategy to mitigate drought, flooding, and sediment transport in drylands. Systems 7:53.

Nicosia, A., Carollo, F.G., Di Stefano, C., Palmeri, V., Pampalone, V., Serio, M.A et al. 2024. The importance of measuring soil erosion by water at the field scale: a review. Water (Basel) 16:3427.

Noto, S., Tauro, F., Petroselli, A., Apollonio, C., Botter, G., Grimaldi, S. 2022. Low-cost stage-camera system for continuous water-level monitoring in ephemeral streams. Hydrol. Sci. J 67:1439-1448.

Palmeri V., Di Stefano C., Nicosia A., Pampalone V., Ferro V. 2024. Terrestrial photogrammetry–GIS methodology for measuring rill erosion at the Sparacia Experimental Area, Sicily. Remote Sens. 16:4232.

Pampalone, V., Serio, M.A., Bagarello, V., Ferro ,V. 2024. Empirical modeling of soil erosion using unit plot data at Sparacia experimental area (southern Italy). J. Soils Sediments 24:2535-2547.

Petroselli A., Tauro F., 2017. Cape Fear: monitoring basic hydrological processes in an outdoor hillslope plot. Environmental Monitoring and Assessment 189, 132.

Sánchez-Crespo, F.A., Gómez-Villarino, M.T., Gallego, E., Fuentes, J.M., García, A.I., Ayuga, F. 2023. Monitoring of water and tillage soil erosion in agricultural basins, a comparison of measurements acquired by differential interferometric analysis of sentinel TopSAR images and a terrestrial LIDAR system. Land 12:408.

Tan, S.S.X., Kuebbing, S.E. 2023. A synthesis of the effect of regenerative agriculture on soil carbon sequestration in Southeast Asian croplands. Agr. Ecosyst. Environ. 349:108450.

Tauro, F., Noto, S., Botter, G., Grimaldi, S. 2022. Assessing the optimal stage-cam target for continuous water level monitoring in ephemeral streams: experimental evidence. Remote Sens. 14: 6064.

Tauro, F., Petroselli, A., Fiori, A., Romano, N., Rulli, M.C., Porfiri, M., et al. 2017. "Cape Fear"– A hybrid hillslope plot for monitoring hydrological processes. Hydrology 4:35.

Tauro, F., Petroselli, A., Grimaldi, S., 2023. Thinking inside the box: Investigating peak storm response in a simplified outdoor slope setup. J. Hydrol. 625:130064.

Todisco, F., Vergni, L., Mannocchi, F., Bomba, C. 2012. Calibration of the soil loss measurement method at the Masse experimental station. Catena 91:4-9.

Vinci, A., Todisco, F., Brigante, R., Mannocchi, F., Radicioni, F. 2017. A smartphone camera for the structure from motion reconstruction for measuring soil surface variations and soil loss due to erosion. Hydrol. Res. 48:673-685.

Žížala, D., Zádorová, T., Kapička, J. 2017. Assessment of soil degradation by erosion based on analysis of soil properties using aerial hyperspectral images and ancillary data, Czech Republic. Remote Sens. 9:28.

Figure 1. Cape Fear experimental plot. General view (left); detail of aluminum tank (center) with the interconnected compartments and the turbidity sensor (right, up and down).

Figure 2. Photo captured at roughly one-meter intervals along the perimeter of Cape Fear's experimental area. In the detail, one of the 14 ground control points.

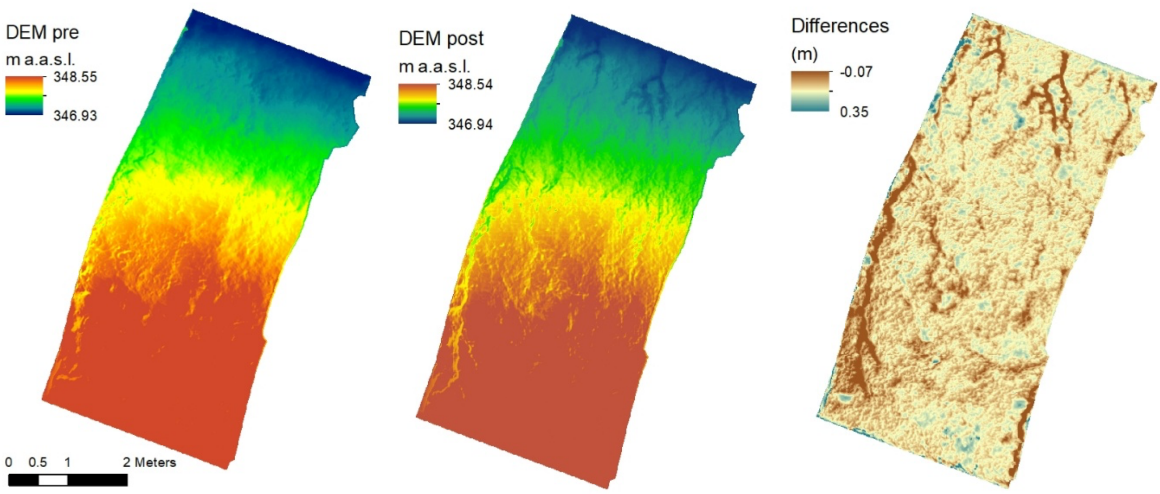

Figure 3. Pre-event DEM (left), post-event DEM (center), differences post-pre-event (right).

Figure 4. Particular of the lower section of the studied area: pre-event condition (left), post-event condition (center), micro-rills detected by image analysis (right).